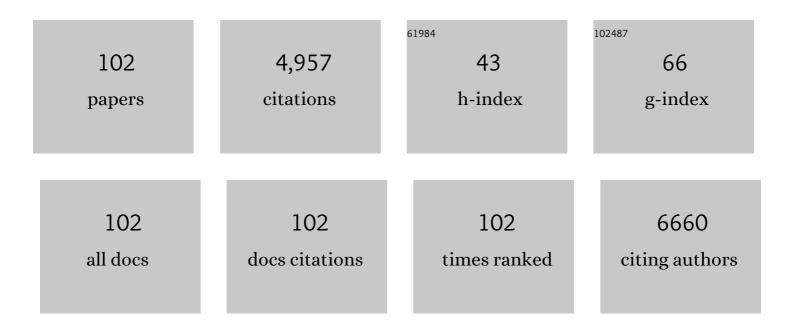
List of Publications by Year in descending order

Source: https://exaly.com/author-pdf/612022/publications.pdf Version: 2024-02-01



\//гінца Нц

#	Article	IF	CITATIONS
1	Sacrificial templating synthesis of metal-organic framework hybrid nanosheets as efficient pre-electrocatalyst for oxygen evolution reaction in alkaline. Colloids and Surfaces A: Physicochemical and Engineering Aspects, 2022, 632, 127745.	4.7	7
2	Amorphous-crystalline cobalt-molybdenum bimetallic phosphide heterostructured nanosheets as Janus electrocatalyst for efficient water splitting. International Journal of Hydrogen Energy, 2022, 47, 7783-7792.	7.1	21
3	Fe-doped Co9S8@CoO aerogel with core-shell nanostructures for boosted oxygen evolution reaction. International Journal of Hydrogen Energy, 2022, 47, 21182-21190.	7.1	16
4	Phosphatizing engineering of heterostructured Rh2P/Rh nanoparticles on doped graphene for efficient hydrogen evolution in alkaline and acidic media. International Journal of Hydrogen Energy, 2022, 47, 24669-24679.	7.1	6
5	Highly Efficient Alkaline Water Splitting with Ruâ€Doped Coâ^'V Layered Double Hydroxide Nanosheets as a Bifunctional Electrocatalyst. ChemSusChem, 2021, 14, 730-737.	6.8	63
6	Rh ₂ P Nanoparticles Partially Embedded in N/P-Doped Carbon Scaffold at Ultralow Metal Loading for High Current Density Water Electrolysis. ACS Applied Nano Materials, 2021, 4, 3369-3376.	5.0	14
7	Mechanism and kinetics of cathodic corrosion of fluorine-doped tin oxide revealed by in situ oblique incident reflectivity difference. Electrochemistry Communications, 2021, 127, 107037.	4.7	5
8	Reusable OIRD Microarray Chips Based on a Bienzyme-Immobilized Polyaniline Nanowire Forest for Multiplexed Detection of Biological Small Molecules. Analytical Chemistry, 2021, 93, 10697-10703.	6.5	11
9	Electronic interaction boosted electrocatalysis of iridium nanoparticles on nitrogen-doped graphene for efficient overall water splitting in acidic and alkaline media. Chemical Engineering Journal, 2021, 415, 129034.	12.7	42
10	Simultaneous phase transformation and doping <i>via</i> a unique photochemical–electrochemical strategy to achieve a highly active Fe-doped Ni oxyhydroxide oxygen evolution catalyst. Journal of Materials Chemistry A, 2021, 9, 4213-4220.	10.3	26
11	Ionic liquid <i>in situ</i> functionalized carbon nanotubes as metal-free catalyst for efficient electrocatalytic hydrogen evolution reaction. Nanoscale, 2021, 13, 4444-4450.	5.6	22
12	Ruâ€Doping Enhanced Electrocatalysis of Metal–Organic Framework Nanosheets toward Overall Water Splitting. Chemistry - A European Journal, 2020, 26, 17091-17096.	3.3	51
13	A microwell array structured surface plasmon resonance imaging gold chip for high-performance label-free immunoassay. Analyst, The, 2020, 145, 6395-6400.	3.5	5
14	Strong Electronic Interaction Enhanced Electrocatalysis of Metal Sulfide Clusters Embedded Metal–Organic Framework Ultrathin Nanosheets toward Highly Efficient Overall Water Splitting. Advanced Science, 2020, 7, 2001965.	11.2	129
15	Transitionâ€Metal Phosphides: Activity Origin, Energyâ€Related Electrocatalysis Applications, and Synthetic Strategies. Advanced Functional Materials, 2020, 30, 2004009.	14.9	309
16	Gold-Incorporated Cobalt Phosphide Nanoparticles on Nitrogen-Doped Carbon for Enhanced Hydrogen Evolution Electrocatalysis. ACS Applied Materials & Interfaces, 2020, 12, 16548-16556.	8.0	55
17	Optical imaging of the potential distribution at transparent electrode/solution interfaces. Chemical Communications, 2020, 56, 4531-4534.	4.1	9
18	Heterostructured CoSe ₂ /FeSe ₂ Nanoparticles with Abundant Vacancies and Strong Electronic Coupling Supported on Carbon Nanorods for Oxygen Evolution Electrocatalysis. ACS Sustainable Chemistry and Engineering, 2020, 8, 4658-4666.	6.7	56

#	Article	IF	CITATIONS
19	Versatile Route To Fabricate Precious-Metal Phosphide Electrocatalyst for Acid-Stable Hydrogen Oxidation and Evolution Reactions. ACS Applied Materials & Interfaces, 2020, 12, 11737-11744.	8.0	37
20	Spatially resolved electrochemical reversibility of a conducting polymer thin film imaged by oblique-incidence reflectivity difference. Chemical Communications, 2020, 56, 1972-1975.	4.1	10
21	Core–shell structured BiOCl@polydopamine hierarchical hollow microsphere for highly efficient photocatalysis. Colloids and Surfaces A: Physicochemical and Engineering Aspects, 2019, 580, 123747.	4.7	17
22	Rational Synthesis of Iron/Nitrogenâ€Đoped Carbon Catalyst through a Spatial Isolation Strategy for Efficient Oxygen Reduction in Acidic and Alkaline Media. Chemistry - A European Journal, 2019, 25, 11560-11565.	3.3	9
23	Effect of nanoparticle composition on oxygen reduction reaction activity of Fe/N–C catalysts: a comparative study. Catalysis Science and Technology, 2019, 9, 711-717.	4.1	23
24	Chip architecture-enabled sensitivity enhancement of oblique-incidence reflectivity difference for label-free protein microarray detection. Sensors and Actuators B: Chemical, 2019, 294, 216-223.	7.8	16
25	Metal-support interaction boosted electrocatalysis of ultrasmall iridium nanoparticles supported on nitrogen doped graphene for highly efficient water electrolysis in acidic and alkaline media. Nano Energy, 2019, 62, 117-126.	16.0	151
26	Benchmarking Three Ruthenium Phosphide Phases for Electrocatalysis of the Hydrogen Evolution Reaction: Experimental and Theoretical Insights. Chemistry - A European Journal, 2019, 25, 7826-7830.	3.3	42
27	Amorphous nickel sulfide nanosheets with embedded vanadium oxide nanocrystals on nickel foam for efficient electrochemical water oxidation. Journal of Materials Chemistry A, 2019, 7, 10534-10542.	10.3	65
28	Efficient oxygen reduction electrocatalysis on Mn3O4 nanoparticles decorated N-doped carbon with hierarchical porosity and abundant active sites. International Journal of Hydrogen Energy, 2019, 44, 26387-26395.	7.1	22
29	Hierarchically porous Fe/N–C hollow spheres derived from melamine/Fe-incorporated polydopamine for efficient oxygen reduction reaction electrocatalysis. Sustainable Energy and Fuels, 2019, 3, 3455-3461.	4.9	25
30	Single-layer graphene-coated gold chip for electrochemical surface plasmon resonance study. Analytical and Bioanalytical Chemistry, 2019, 411, 4577-4585.	3.7	2
31	Ultrasmall Ru ₂ P nanoparticles on graphene: a highly efficient hydrogen evolution reaction electrocatalyst in both acidic and alkaline media. Chemical Communications, 2018, 54, 3343-3346.	4.1	102
32	One-Pot Synthesis of Co/CoFe ₂ O ₄ Nanoparticles Supported on N-Doped Graphene for Efficient Bifunctional Oxygen Electrocatalysis. ACS Sustainable Chemistry and Engineering, 2018, 6, 3556-3564.	6.7	85
33	Electrochemically enhanced antibody immobilization on polydopamine thin film for sensitive surface plasmon resonance immunoassay. Talanta, 2018, 182, 470-475.	5.5	24
34	Mesoporous Hollow Nitrogen-Doped Carbon Nanospheres with Embedded MnFe ₂ O ₄ /Fe Hybrid Nanoparticles as Efficient Bifunctional Oxygen Electrocatalysts in Alkaline Media. ACS Applied Materials & Interfaces, 2018, 10, 20440-20447.	8.0	73
35	Single-layer graphene-coated gold chip for enhanced SPR imaging immunoassay. Sensors and Actuators B: Chemical, 2018, 273, 1548-1555.	7.8	21
36	Manganese/Cobalt Bimetal Nanoparticles Encapsulated in Nitrogen-Rich Graphene Sheets for Efficient Oxygen Reduction Reaction Electrocatalysis. ACS Sustainable Chemistry and Engineering, 2018, 6, 10545-10551.	6.7	28

#	Article	IF	CITATIONS
37	Fenton-Reaction-Derived Fe/N-Doped Graphene with Encapsulated Fe3C Nanoparticles for Efficient Photo-Fenton Catalysis. Catalysis Letters, 2018, 148, 2528-2536.	2.6	8
38	Molybdenum carbide/phosphide hybrid nanoparticles embedded P, N co-doped carbon nanofibers for highly efficient hydrogen production in acidic, alkaline solution and seawater. Electrochimica Acta, 2018, 281, 710-716.	5.2	53
39	Ru ₂ P Nanoparticle Decorated P/N-Doped Carbon Nanofibers on Carbon Cloth as a Robust Hierarchical Electrocatalyst with Platinum-Comparable Activity toward Hydrogen Evolution. ACS Applied Energy Materials, 2018, 1, 3143-3150.	5.1	49
40	Bifunctional polydopamine thin film coated zinc oxide nanorods for label-free photoelectrochemical immunoassay. Talanta, 2017, 166, 141-147.	5.5	27
41	Fe/Fe3C nanoparticles loaded on Fe/N-doped graphene as an efficient heterogeneous Fenton catalyst for degradation of organic pollutants. Colloids and Surfaces A: Physicochemical and Engineering Aspects, 2017, 518, 145-150.	4.7	48
42	A fluorescence aptasensor based on semiconductor quantum dots and MoS2 nanosheets for ochratoxin A detection. Sensors and Actuators B: Chemical, 2017, 246, 61-67.	7.8	104
43	Cobalt nanoparticle decorated graphene aerogel for efficient oxygen reduction reaction electrocatalysis. International Journal of Hydrogen Energy, 2017, 42, 5930-5937.	7.1	28
44	One-pot synthesis of Co/N-doped mesoporous graphene with embedded Co/CoO _x nanoparticles for efficient oxygen reduction reaction. Nanoscale, 2017, 9, 10233-10239.	5.6	69
45	Nitrogen/sulfur-doping of graphene with cysteine as a heteroatom source for oxygen reduction electrocatalysis. Journal of Colloid and Interface Science, 2017, 505, 32-37.	9.4	44
46	A Bioinspired Surface Chemistry for Solid-State Nanopores Modification. Biophysical Journal, 2017, 112, 458a.	0.5	0
47	In Situ Investigation of Electrochemically Mediated Surface-Initiated Atom Transfer Radical Polymerization by Electrochemical Surface Plasmon Resonance. Analytical Chemistry, 2017, 89, 4355-4358.	6.5	14
48	Interfacial Separation-Enabled All-Dry Approach for Simultaneous Visualization, Transfer, and Enhanced Raman Analysis of Latent Fingerprints. ACS Applied Materials & Interfaces, 2017, 9, 37350-37356.	8.0	7
49	Polydopamine thin film-assisted patterned chemical bath deposition of ZnO nanorods on arbitrary substrates. CrystEngComm, 2017, 19, 6182-6188.	2.6	4
50	Protein immobilization and fluorescence quenching on polydopamine thin films. Journal of Colloid and Interface Science, 2016, 477, 123-130.	9.4	33
51	Patterning of Metal Films on Arbitrary Substrates by Using Polydopamine as a UV-Sensitive Catalytic Layer for Electroless Deposition. Langmuir, 2016, 32, 5285-5290.	3.5	40
52	Fe3C nanoparticle decorated Fe/N doped graphene for efficient oxygen reduction reaction electrocatalysis. Journal of Power Sources, 2016, 332, 305-311.	7.8	104
53	Simultaneous Transfer and Imaging of Latent Fingerprints Enabled by Interfacial Separation of Polydopamine Thin Film. Analytical Chemistry, 2016, 88, 10357-10361.	6.5	17
54	Iron oxide/oxyhydroxide decorated graphene oxides for oxygen reduction reaction catalysis: a comparison study. RSC Advances, 2016, 6, 29848-29854.	3.6	38

#	Article	IF	CITATIONS
55	First-principles study of SF6 decomposed gas adsorbed on Au-decorated graphene. Applied Surface Science, 2016, 367, 259-269.	6.1	141
56	Competitive Immunoassays Using Antigen Microarrays. Methods in Molecular Biology, 2016, 1368, 237-247.	0.9	3
57	Experimental Sensing and Density Functional Theory Study of H ₂ S and SOF ₂ Adsorption on Auâ€Modified Graphene. Advanced Science, 2015, 2, 1500101.	11.2	213
58	Bioinspired synthesis of nitrogen/sulfur co-doped graphene as an efficient electrocatalyst for oxygen reduction reaction. Journal of Power Sources, 2015, 279, 252-258.	7.8	117
59	Colorimetric detection of mercury(II) based on 2,2′-bipyridyl induced quasi-linear aggregation of gold nanoparticles. Sensors and Actuators B: Chemical, 2015, 215, 421-427.	7.8	36
60	Multi-color quantum dot-based fluorescence immunoassay array for simultaneous visual detection of multiple antibiotic residues in milk. Biosensors and Bioelectronics, 2015, 72, 320-325.	10.1	173
61	Solvent-mediated directionally self-assembling MoS ₂ nanosheets into a novel worm-like structure and its application in sodium batteries. Journal of Materials Chemistry A, 2015, 3, 9932-9937.	10.3	74
62	Spontaneous interfacial reaction between metallic copper and PBS to form cupric phosphate nanoflower and its enzyme hybrid with enhanced activity. Colloids and Surfaces B: Biointerfaces, 2015, 135, 613-618.	5.0	69
63	Stabilization of gold nanoparticles on glass surface with polydopamine thin film for reliable LSPR sensing. Journal of Colloid and Interface Science, 2015, 460, 258-263.	9.4	34
64	Adsorptions of SO2, SOF2, and SO2F2 on Pt-modified anatase (101) surface: Sensing mechanism study. Applied Surface Science, 2015, 353, 662-669.	6.1	12
65	Hybrid ZnO Nanorodâ€Polymer Brush Hierarchically Nanostructured Substrate for Sensitive Antibody Microarrays. Advanced Materials, 2015, 27, 181-185.	21.0	67
66	One-step synthesis of monodisperse gold dendrite@polypyrrole core-shell nanoparticles and their enhanced catalytic durability. Colloid and Polymer Science, 2015, 293, 505-512.	2.1	8
67	Multifunctionalized reduced graphene oxide-doped polypyrrole/pyrrolepropylic acid nanocomposite impedimetric immunosensor to ultra-sensitively detect small molecular aflatoxin B1. Biosensors and Bioelectronics, 2015, 63, 185-189.	10.1	93
68	DNAâ€Templated Biomimetic Enzyme Sheets on Carbon Nanotubes to Sensitively In Situ Detect Superoxide Anions Released from Cells. Advanced Functional Materials, 2014, 24, 5897-5903.	14.9	59
69	DNAâ€Promoted Ultrasmall Palladium Nanocrystals on Carbon Nanotubes: Towards Efficient Formic Acid Oxidation. ChemElectroChem, 2014, 1, 72-75.	3.4	19
70	Dual signal amplification of surface plasmon resonance imaging for sensitive immunoassay of tumor marker. Analytical Biochemistry, 2014, 453, 16-21.	2.4	35
71	ZnO nanorod–templated well-aligned ZrO ₂ nanotube arrays for fibroblast adhesion and proliferation. Nanotechnology, 2014, 25, 215102.	2.6	12
72	A high performance xylose microbial fuel cell enabled by Ochrobactrum sp. 575 cells. RSC Advances, 2014, 4, 39839-39843.	3.6	14

#	Article	IF	CITATIONS
73	Graphene oxide-enabled tandem signal amplification for sensitive SPRi immunoassay in serum. Chemical Communications, 2014, 50, 2133.	4.1	45
74	Polydopamine-Functionalization of Graphene Oxide to Enable Dual Signal Amplification for Sensitive Surface Plasmon Resonance Imaging Detection of Biomarker. Analytical Chemistry, 2014, 86, 4488-4493.	6.5	127
75	Sensitive detection of multiple mycotoxins by SPRi with gold nanoparticles as signal amplification tags. Journal of Colloid and Interface Science, 2014, 431, 71-76.	9.4	45
76	ZnO Nanomulberry and Its Significant Nonenzymatic Signal Enhancement for Protein Microarray. ACS Applied Materials & Interfaces, 2014, 6, 7728-7734.	8.0	20
77	Adsorption of SF6 decomposed gas on anatase (101) and (001) surfaces with oxygen defect: A density functional theory study. Scientific Reports, 2014, 4, 4762.	3.3	28
78	A DFT study of SF6 decomposed gas adsorption on an anatase (101) surface. Applied Surface Science, 2013, 286, 47-53.	6.1	42
79	Sensitive competitive immunoassay of multiple mycotoxins with non-fouling antigen microarray. Biosensors and Bioelectronics, 2013, 50, 338-344.	10.1	66
80	Electroanalysis in micro- and nano-scales. Journal of Electroanalytical Chemistry, 2013, 688, 20-31.	3.8	36
81	A portable flow-through fluorescent immunoassay lab-on-a-chip device using ZnO nanorod-decorated glass capillaries. Lab on A Chip, 2013, 13, 1797.	6.0	47
82	Fluorescent immunoassay system. , 2013, , .		0
83	Interface Functionalization of Photoelectrodes with Graphene for High Performance Dyeâ€Sensitized Solar Cells. Advanced Functional Materials, 2012, 22, 5245-5250.	14.9	135
84	Thermoelectric Bi ₂ Te ₃ -improved charge collection for high-performance dye-sensitized solar cells. Energy and Environmental Science, 2012, 5, 6294-6298.	30.8	77
85	Rewritable multicolor fluorescent patterns for multistate memory devices with high data storage capacity. Chemical Communications, 2011, 47, 9609.	4.1	55
86	Interaction mechanisms of CdTe quantum dots with proteins possessing different isoelectric points. MedChemComm, 2011, 2, 283.	3.4	29
87	Highly sensitive poly[glycidyl methacrylate-co-poly(ethylene glycol) methacrylate] brush-based flow-through microarray immunoassay device. Biomedical Microdevices, 2011, 13, 769-777.	2.8	38
88	ZnO nanorods-enhanced fluorescence for sensitive microarray detection of cancers in serum without additional reporter-amplification. Biosensors and Bioelectronics, 2011, 26, 3683-3687.	10.1	69
89	Nanomaterialâ€based advanced immunoassays. Wiley Interdisciplinary Reviews: Nanomedicine and Nanobiotechnology, 2011, 3, 119-133.	6.1	30
90	Bifunctional electro-optical nanoprobe to real-time detect local biochemical processes in single cells. Biosensors and Bioelectronics, 2011, 26, 4484-4490.	10.1	48

#	Article	IF	CITATIONS
91	Sensitive protein microarray synergistically amplified by polymer brush-enhanced immobilizations of both probe and reporter. Journal of Colloid and Interface Science, 2011, 360, 593-599.	9.4	24
92	Poly[oligo(ethylene glycol) methacrylateâ€ <i>co</i> â€glycidyl methacrylate] Brush Substrate for Sensitive Surface Plasmon Resonance Imaging Protein Arrays. Advanced Functional Materials, 2010, 20, 3497-3503.	14.9	90
93	Fabrication of oriented poly-l-lysine/bacteriorhodopsin-embedded purple membrane multilayer structure for enhanced photoelectric response. Journal of Colloid and Interface Science, 2010, 344, 150-157.	9.4	19
94	GOLD NANOPARTICLE-INCORPORATED POLYELECTROLYTE MULTILAYER FOR SENSITIVE ELECTROCHEMICAL IMMUNOSENSING. Cosmos, 2010, 06, 197-205.	0.4	0
95	In Situ Surface Plasmon Resonance Investigation of the Assembly Process of Multiwalled Carbon Nanotubes on an Alkanethiol Self-Assembled Monolayer for Efficient Protein Immobilization and Detection. Langmuir, 2010, 26, 8386-8391.	3.5	51
96	Randomly Oriented ZnO Nanorods As Advanced Substrate for High-Performance Protein Microarrays. ACS Applied Materials & Interfaces, 2010, 2, 1569-1572.	8.0	47
97	Photografted poly(methyl methacrylate)-based high performance protein microarray for hepatitis B virus biomarker detection in human serum. MedChemComm, 2010, 1, 132.	3.4	37
98	Electrochemically polymerized nanostructured poly(3.4-ethylenedioxythiophene)-poly(styrenesulfonate) buffer layer for a high performance polymer solar cell. Energy and Environmental Science, 2010, 3, 1580.	30.8	34
99	High performance protein microarrays based on glycidyl methacrylate-modified polyethylene terephthalate plastic substrate. Talanta, 2009, 77, 1165-1171.	5.5	36
100	An in situ electrochemical surface plasmon resonance immunosensor with polypyrrole propylic acid film: Comparison between SPR and electrochemical responses from polymer formation to protein immunosensing. Biosensors and Bioelectronics, 2008, 23, 1055-1062.	10.1	81
101	Poly(pyrrole-co-pyrrole propylic acid) film and its application in label-free surface plasmon resonance immunosensors. Analytica Chimica Acta, 2008, 630, 67-74.	5.4	54
102	In Situ Studies of Protein Adsorptions on Poly(pyrrole-co-pyrrole propylic acid) Film by Electrochemical Surface Plasmon Resonance. Langmuir, 2007, 23, 2761-2767.	3.5	82